University of Baghdad
College of Engineering
JOURNAL OF ENGINEERING

Journal of Engineering

journal homepage: www.jcoeng.edu.iq

Volume 30 Number 7 July 2024

Numerical Simulation of the Behaviour of RC T-Beams Strengthened by EB-CFRP Composites Under Bending and Shear Effects

Hasan Ehssan Alobaidi [1,*], Alaa Hussein Al-Zuhairi[2]

Department of Civil Engineering, College of Engineering, University of Baghdad, Baghdad, Iraq
hasan.alobaidi2001m@coeng.uobaghdad.edu.iq[1] , alaalwn@coeng.uobaghdad.edu.iq[2]

ABSTRACT

This article presents the results of numerical simulations performed using ABAQUS/CAE version 2019 .The study aims to evaluate the structural integrity of reinforced concrete (RC) T-beams strengthened with externally bonded carbon fiber reinforcements polymer composite materials (EB) (CFRP), especially their response to bending and shear forces .The numerical model was validated by comparing the numerical and experimental results of eight RC T-beams .The numerical analysis was then extended to include various factors, including the impact of the tilt angle of the U-CFRP shell on the shear strength .The goal of this numerical extension is to implement a numerical model capable of simulating the nonlinear behavior of these beams accurately. A comparative analysis is also performed on the experimental and computational models, focusing on the damage modes and their load-induced deformation characteristics .The results showed a satisfactory level of agreement between the two sides .The average ratio of ultimate load to deflection in the numerical model simulation and experimental beam test is 1.004 and 1.046 ,respectively. The main finding is that inclined U-CFRP deformed at a 45° angle exhibits greater shear stiffness than beams embedded with vertical CFRP panels at a 90° angle, maintaining a constant CFRP panel spacing.

Keywords: T-beams, EB-CFRP, ABAQUS, Nonlinear behavior, Structural performance

*Corresponding author
Peer review under the responsibility of University of Baghdad.
https://doi.org/10.31026/j.eng.2024.07.04

Article received: 16/09/2023
Article accepted: 10/11/2023
Article published: 01/07/2024

المحاكات العددية لسلوك للعتبات الخرسانية المسلحة ذات المقطع T والمقواة بمركبات EB-CFRP تحت تأثيرات الانحناء والقص

حسن احسان العبيدي*، علاء حسين الزهيري

قسم الهندسة المدنية ، كلية الهندسة، جامعة بغداد، بغداد، العراق

الخلاصة

يعرض هذا البحث نتائج المحاكاة العددية التي أجريت باستخدام برنامج العناصر المحدودة المعروف ABAQUS/CAE الإصدار 2019. الهدف من هذه الدراسة هو دراسة الاستجابة الانشائية للعتبات الخرسانية ذات المقطع T المسلحة التي تم تعزيزها بمركبات البوليمر المقوى بألياف الكربون الخارجية (CFRP)(EB)، وتحديداً تحت تأثير قوى الانحناء والقص. تضمنت عملية التحقق العددي التحليل العددي ومقارنة النتائج مع النتائج التجريبية لثمانية عتبات ذات المقطع T من الخرسانة المسلحة. وبعد ذلك، تم توسيع نطاق التحليل العددي ليشمل فحص عدة عوامل، بما في ذلك تأثير زاوية ميل صفائح U-CFRP داخل مجموعة القص. الهدف من هذه الدراسة هو تقديم نموذج عددي يمكنه محاكاة السلوك غير الخطي للعتبات بدقة. تقدم هذه الدراسة مقارنة بين النماذج الحسابية والعملية من حيث سلوك انحراف الحمل وأنماط التشقق، مما يسلط الضوء على اتفاق جيد بين الاثنين. وقد وجد أن متوسط نسبة الحمل النهائي والانحرافات بين نماذج المحاكاة العددية والاختبارات التجريبية للعتبات هي 1.004 و 1.046 على التوالي. تشير نتائج الدراسة إلى أن العتبات التي تتضمن صفائح CFRP المائلة بزاوية 45 درجة تظهر صلابة قص أكبر مقارنة بالعتبات التي تتضمن صفائح CFRP عمودية بزاوية 90 درجة، على افتراض وجود مسافة متساوية بين صفائح CFRP.

الكلمات المفتاحية: عتبات تي, EB-CFRP , اباكوس, التصرف اللاخطي, الاداء الهيكلي.

1. INTRODUCTION

In the last 30 years, carbon fibre-reinforced polymer (CFRP) products have been used to strengthen reinforced concrete (RC) parts. It was a captivating technique for rehabilitating infrastructure. CFRP strengthening has versatile applications, such as constructing new buildings and restoring existing ones **(Abdulhameed and Said, 2019; Abbas and Al-Zuhairi, 2023).** In addition to examining the overall failure criteria of (CFRP)-RC beams, some scholars investigated the localized behavior occurring close to the bond area. Considerable efforts were undertaken to fully understand the behavior of bonds at the interface, particularly in relation to early failures **(Mhanna et al., 2019; Daraj and Al-Zuhairi, 2023)**. Strengthening using FRP composite materials is versatile because it may be employed on various structural elements, such as beams, columns, slabs, and walls. The enhancement may include one or many objectives depending on the individual's classification. Many objectives focus on enhancing the load capacities of a structure, including axial, flexural, and shear loads. Another goal is to improve stiffness to minimize deflections when subjected to service and design loads. Additionally, efforts were made to extend the fatigue life of the structure and enhance its durability against environmental factors **(Buyukozturk et al., 2004; Hernoune et al., 2020; Ibrahim and Al-Zuhairi, 2022)**.

The contact bond is of utmost importance in most cases. It is crucial in transmitting stresses from pre-existing concrete structures to externally attached CFRP materials. The

requirement of an ideal bond length is another factor that limits the attainment of maximum tensile strength activation in CFRP materials. The primary cause of early debonding is the localized concentration of shear strain. However, determining the effective bond lengths might exhibit significant variability due to the divergent criteria and materials used by various researchers in their experimental investigations. For example, in CFRP-to-concrete joints with widths of 25 mm, the bond lengths for 1-ply and 2-ply configurations are 80 and 220 mm, respectively **(Bizindavyi and Neale, 1999)**, 100 mm **(Ueda et al., 1999)**, 80 mm **(Lorenzis et al., 2001)**, and 64-135 mm **(Nakaba et al., 2001)**.

(Deniaud and Roger Cheng, 2003) conducted a comprehensive investigation on the interplay among concrete, steel ties, and fiber-reinforced polymer (FRP) sheets to determine the structural soundness of RC beams under shear stresses. The empirical findings indicate that incorporating FRP reinforcement significantly enhances the maximum shear strength from 15.4% to 42.2% compared with the beams without FRP reinforcement. The increased shear capacity depends on the type of FRP material and the amount of internal shear reinforcement.

(Benzeguir et al., 2019) reports experimental results from 18 RC T-beam samples of different sizes .They examined how the dimensions affect the shear strength of concrete when RC beams reinforced with externally bonded CFRP (EB) panels fail. There is a relationship between the size of concrete, CFRP panels, and shear capacity. **(Zaki et al., 2020)** conducted a series of studies, including the production and testing of five full-scale T-beams, to determine the extent to which CFRP improves the beam's bending strength . Experimental results show that CFRP bending plates connected to CFRP anchors can increase the bending capacity of RC T beams .Performance improves proportionally to the quantity and quality of CFRP anchors until the section reaches its maximum bearing capacity. The ultimate load increases when the anchors are close together.

(Al Shboul et al., 2021) thoroughly studied the behavior of reinforced lightweight and standard-weight concrete beams reinforced with EB high-modulus carbon fibre. A methodological framework included experimental techniques and analytical and computational assessments. The results indicate that more layers enhance the flexural capacity of conventional concrete beams. Even with more than two layers, lightweight beam use has a consistent pattern, according to empirical findings. **(Abbasi et al., 2022)** performed a numerical investigation to evaluate the impact of dimensions on the shear capacity of RC beams reinforced using EB-CFRP. Due to the limited experimental research, only a few finite element (FE) studies consider the size impact. The findings demonstrate that numerical simulations can accurately forecast experimental outcomes. Additionally, the shear strength of concrete and the contribution of CFRP to shear resistance decrease when the size of beams increases. **(Najaf et al., 2022)** simulated a concrete beam using the FE software ABAQUS and examined the effects of FRP type, amount, and installation angle. The results show that when the quantity of sheets and installation distance are maintained constant, FRP sheets at a 45° installation angle reduce displacement more than those at 60°. This effect is greater when the installation angle is 60° instead of 90°. Plates lower the middle beam span's greatest lateral strain by 12.5%. Prestressed (FRP) sheets strengthen specimens. The load grows until compressive concrete smashing breaks the beam.

This effort created a numerical model that correctly simulates the experiment. T-reinforced concrete beams strengthened for flexural and shear resistance were studied. The main objective was to determine how two parameters affected final bearing capacity and deflection. The influence of CFRP laminate width in the flexural group and U-CFRP sheet spacing in the shear group was evaluated. The experimental data confirmed the theoretical

conclusions, which were used to conduct parametric studies on the U-CFRP sheet inclination angle's effect on shear strength.

2. TESTED SPECIMENS

Numerical simulation was conducted on the experimental results of **(Alobaidi and Al-Zuhairi, 2023)** on eight RC T beams, including two reference beams that are not subjected to any form of strengthening and six strengthened beams. These beams are categorized into two primary groups based on the type of strengthening applied: flexural and shear strengthening. The primary variable selected for the flexural group was CFRP laminate width, and that for the shear group was U-CFRP sheet spacing. **Figs. 1 and 2** show the details of the flexural and shear group beams, respectively. **Table 1.** shows the details of the tested beams.

Table 1. Details of the tested beams.

Group	CFRP Type	Beam-ID	Laminated or sheet CFRP width (mm)	U-CFRP Sheet spacing (mm)
Shear	U-wrap sheet	Ref.(BS.C)	-	-
		BS.S1	100	166
		BS.S2	100	125
		BS.S3	100	100
Flexural	Laminated	Ref.(BF.C)	-	-
		BF.S1	50	-
		BF.S2	100	-
		BF.S3	150	-

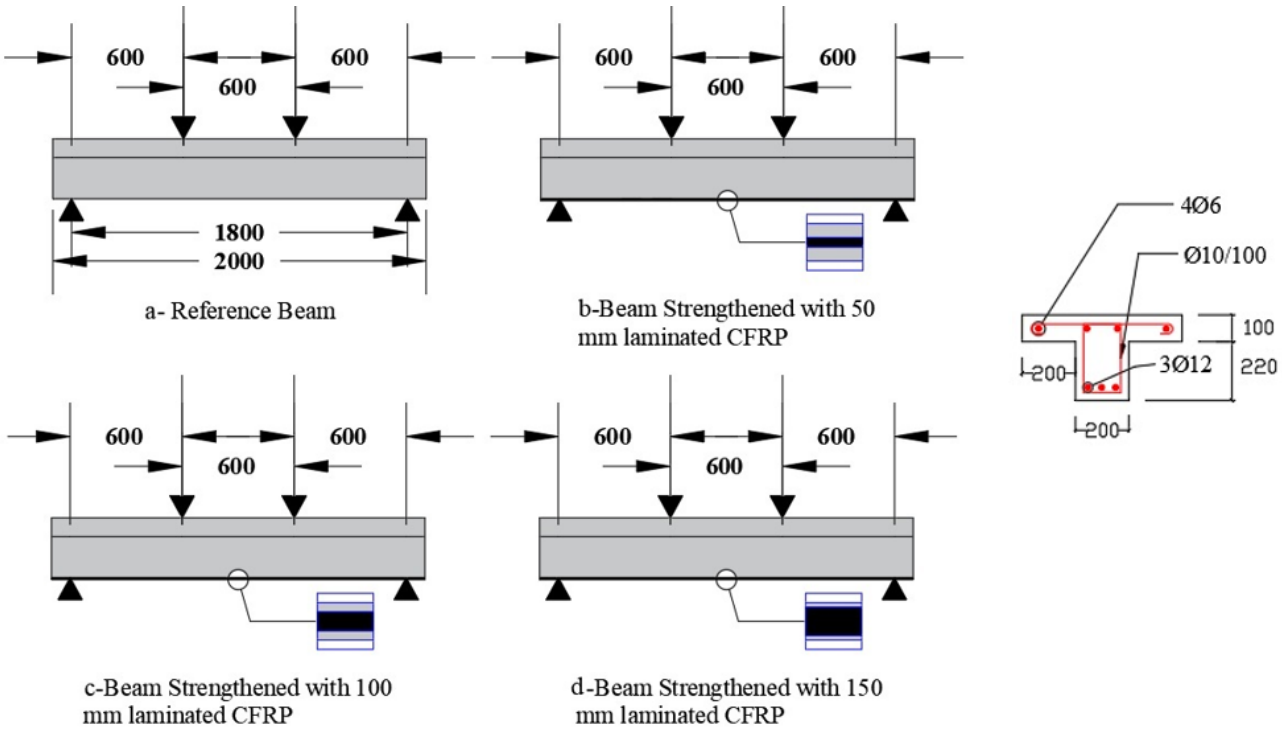

Figure 1. Details of beams for the flexural group.

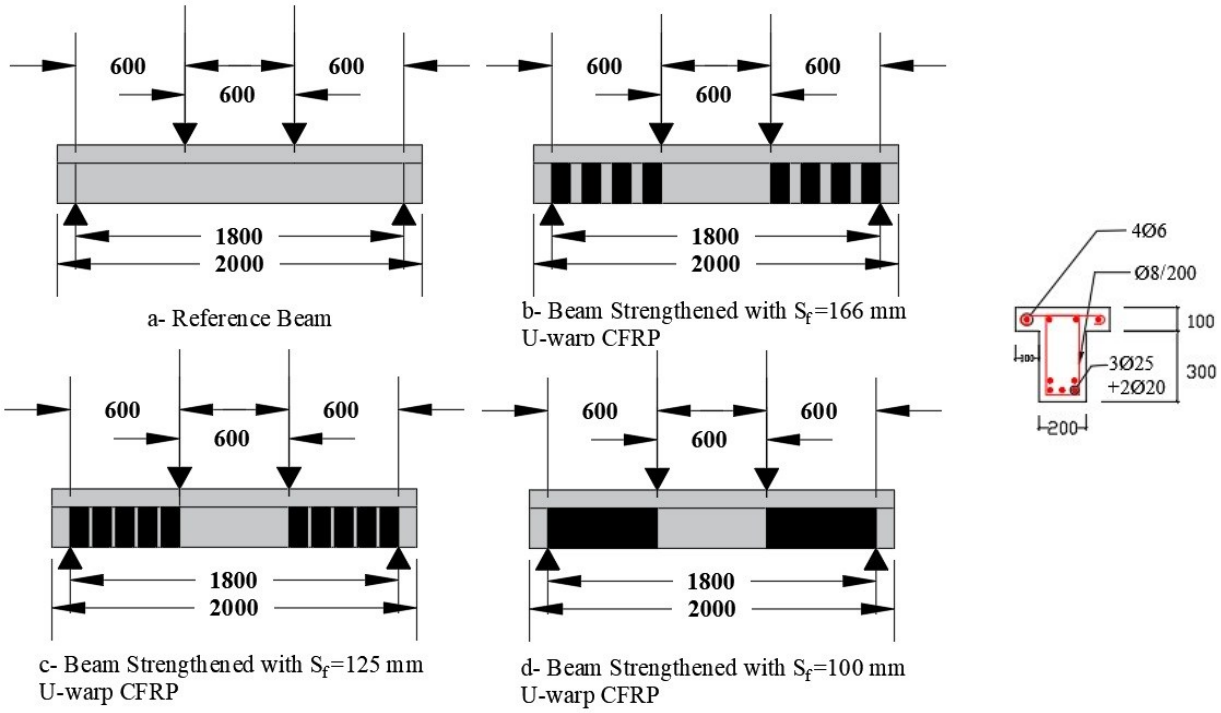

Figure 2. Details of beams for the shear group.

The physical characteristics of concrete, such as its modulus of elasticity (24.405 GPa), compressive strength (f'_c=26.96 MPa), and splitting tensile strength (2.9 MPa) were measured. **Table 2** provides the reinforcement steel properties employed in this study. For the carbon fibre fabrics, the manufacturer/supplier provided their properties (mechanical and physical), including the nominal thickness of 0.012 and 0.166 mm, a tensile strength of 3100 and 4900 MPa, and an ultimate elongation value of 0.018% and 2.1% for the laminate and CFRP sheet, respectively. The modulus of elasticity was equal to 170000 MPa for the laminate and 230000 MPa for the CFRP sheet.

Table 2. Tensile characteristics of the steel reinforcement bars.

Diameter (mm)	Measured Diameter (mm)	Area (mm^2)	Mean Yield Ten. Stress, fy (MPa)	Mean Ultimate Ten. Strength, fu (MPa)	Elongation (%)
6	6	28.26	580	650	12.4
8	8	50.3	523	662	12.4
10	10	78.5	508.70	647.43	15.90
12	12	113.04	470.03	623.3	19.50
20	20	314	671.61	686.32	13.80
25	25	490.6	572.4	724.9	17.6

3. MODELLING AND ANALYSIS OF TESTED BEAMS

The FE method in the standard model implemented by the ABAQUS 2019 PC program was used to analyze the T-beams. The structure of all beams was studied using a single-step approach, specifically, static analysis. The concrete material properties were accurately

represented by simulating the T-beams using the isoperimetric eight-node brick element (C3D8R). The truss element (T3D2), a two-node bar element that can undergo 3D displacement in the x, y, and z axes, was utilized for the reinforced steel bars. 2D shell elements (specifically, the S4R element) represented the CFRP laminates or sheets. This element type is characterised by its ability to accurately model doubly curved thin or thick shells using decreased integration and hourglass control and to account for finite membrane stresses. Many components were generated to thoroughly analyze all the specimens inside the ABAQUS environmental framework, as shown in **Figs. 3 and 4.**

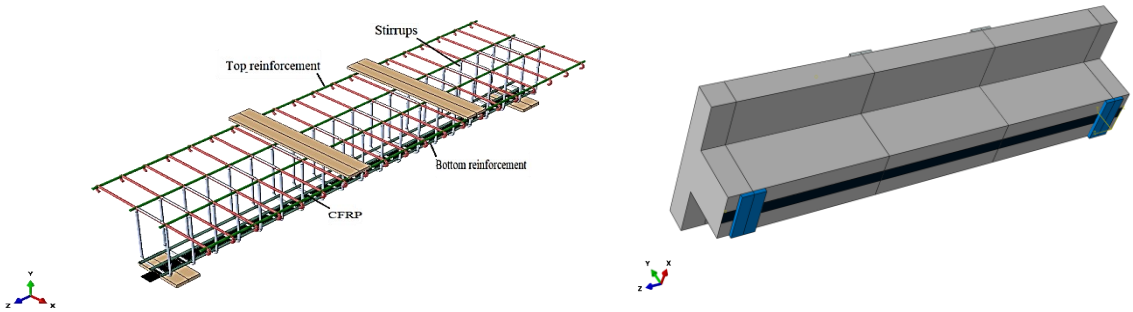

Figure 3. Creating parts and assembly in ABAQUS (flexural group).

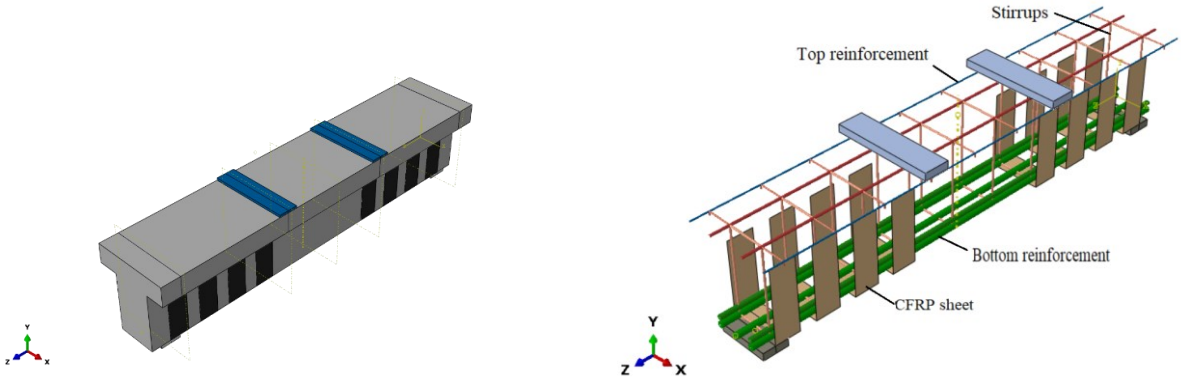

Figure 4. Creating parts and assembly in ABAQUS (shear group).

The simple support at one edge of the beam was simulated as a hinge by restricting the nodes along one line of supporting plate in tandem with the beam soffit's breadth in the local x and y directions (Ux=Uy=0). By contrast, the other support was treated as a roller by restricting the y-direction (Uy=0) and permitting longitudinal motions and rotations around the x-axis. **Fig. 5** shows the boundary conditions and load definitions.

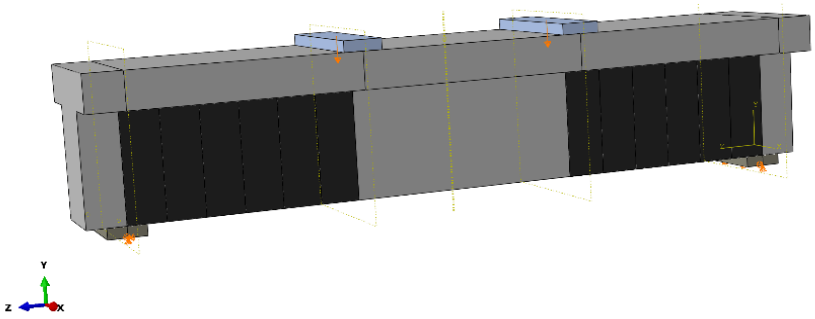

Figure 5. Boundary and loading circumstances were utilized in the study.

The reinforcement was considered entirely embedded in concrete to evaluate complete interaction. The tie constraint option was employed to connect two distinct surfaces, the master concrete surface, and the slave CFRP surface, to ensure the absence of any relative motion between them. The concrete compressive and tensile strength were illustrated in **Tables 3 and 4** based on the studies of **(Elwi and Murray, 1979; Hordijk and Reinhardt, 1991)**, respectively. **Table 5** presents the input data material for concrete plasticity properties.

Table 3. Concrete tension data.

Yield Stress (MPa)	Strain	Yield Stress (MPa)	Strain
2.884612219	0	0.364194973	0.35
1.543950159	0.066	0.309742761	0.39
0.724678029	0.173	0.258016029	0.43
0.585226723	0.220	0.197711839	0.48
0.424973995	0.308		

Table 4. Concrete compressive data.

Yield Stress (MPa)	Inelastic Strain	Yield Stress (MPa)	Inelastic Strain
15.3932053	6.82145E-05	18.3474223	0.003243174
19.77700117	0.00015034	15.96977367	0.003844604
23.10369328	0.000274225	13.92255819	0.004429493
25.33340322	0.000439944	7.550443848	0.007165604
26.58638871	0.000650361	4.580199845	0.009807316
26.96000000	0.000895255	3.057635463	0.012374707
25.94595563	0.001431808	2.187935329	0.014885345
23.63624367	0.002030453	1.633015996	0.017428084
20.94190522	0.00264186	1.266401123	0.019948106

Table 5. Input data for concrete.

Young's modulus	24405
Poisson ratio	0.2
Dilation angle	36
Eccentricity	0.1
$\epsilon_{bo}/\epsilon_{co}$	1.16
k_c	0.667
Viscosity parameter	0

Mesh sensitivity, shown in **Fig. 6,** indicated that as long as the components were more significant than the aggregate size and showed reasonable agreement with the test results. No considerable sensitivity to the mesh size was observed. Therefore, for efficient computation, the mesh size of 25.0 mm with an aspect ratio of (1), as shown in **Fig. 7**

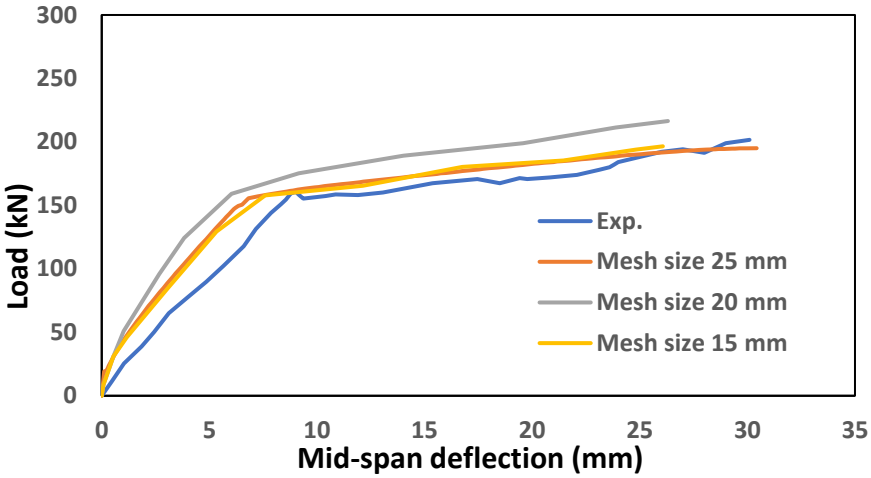

Figure 6. Mesh sensitivity study.

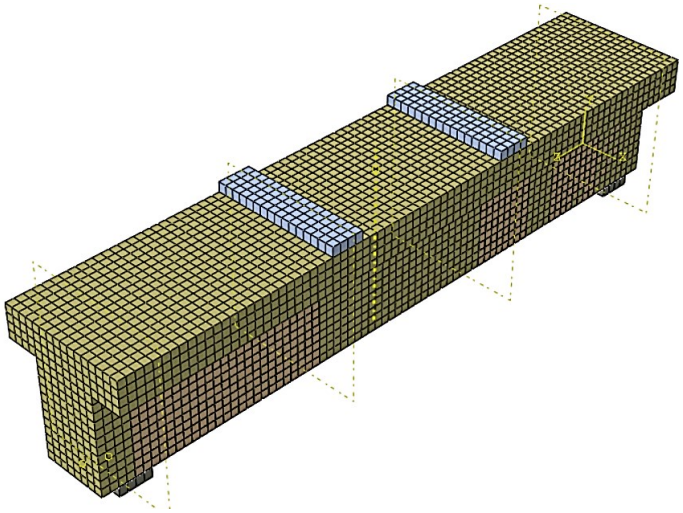

Figure 7. Numerical meshed model.

4. RESULTS AND DISCUSSION

4.1 Calibration of the Fabricated FE model

Figs. 8 and 9 depict the comparison of load-deflection relationship between the experimental and numerical findings for the flexural and shear groups, respectively.

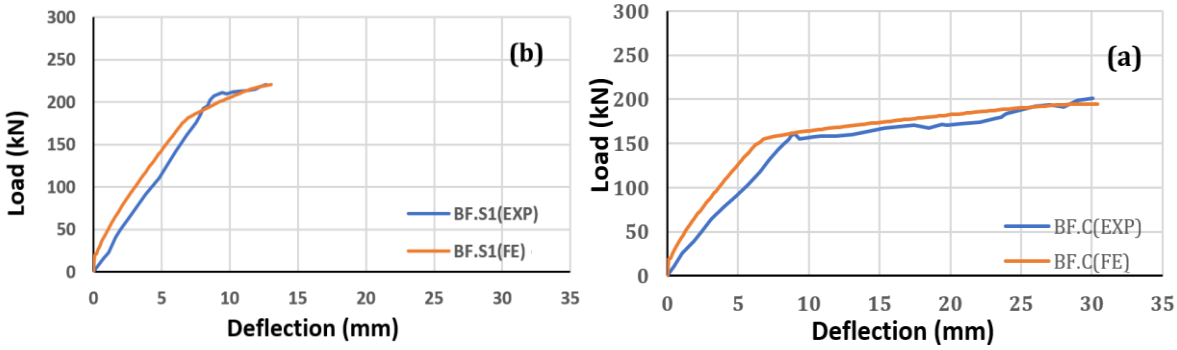

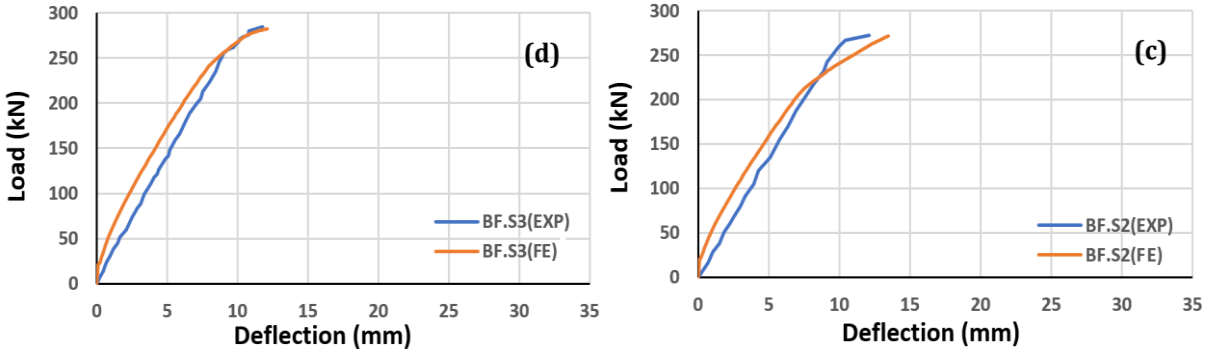

Figure 8. Experimental and numerical load-deflection relationship for the beams (flexural group); a) BF.C beam, b) BF.S1 beam, c) BF.S2 beam, d) BF.S3 beam

FE study showed that models were stiffer than experimental samples. Based on load-deflection relations under applied stresses, this result is drawn. Many factors lead FEM results to be stiffer. Concrete microcracks from drying, shrinkage, and curing were seen throughout the experiment. Thus, the specimen may have less stiffness than the FE study indicated. **(Singh et al., 2017; Raza et al., 2020; Naqi and Al-Zuhair, 2020; Abdulhameed et al., 2022)**.

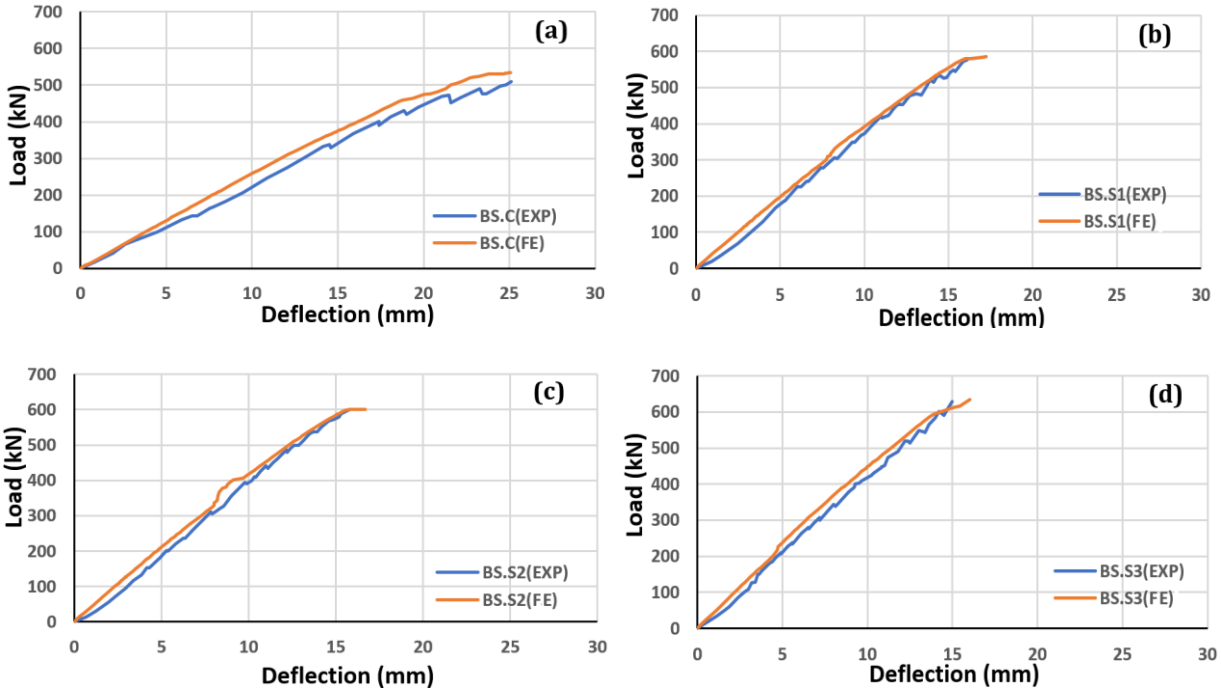

Figure 9. Experimental and numerical load–deflection relationship for the beams (shear group), a) BS.C beam, b) BS.S1 beam, c) BS.S2 beam, d) BS.S3 beam

This study compared experimental and FE model peak load stage ultimate load and deflection. All static-tested beams were analyzed. Experimental and computer models' ultimate load and deflection were strongly correlated. The average value and coefficient of variation for ultimate load ratio (Pu)FE/(Pu)Exp were 1.004 and 2.216%, respectively. The average and coefficient of variation for the deflection ratio (δ FE/δ Exp) were 1.046 and

3.584%, respectively. As explained in **Table 6.** Therefore, FE analysis is a superior and dependable approach for modelling the nonlinear characteristics of RC T beams using CFRP.

4.2 Crack Patterns

According to the principles of continuum damage mechanics, a damage model must be used in conjunction with a plasticity model. accurate methodologies and techniques must be employed to accurately predict and simulate the behaviour of concrete **(Nicolaides and Markou, 2015; Zhang et al., 2016; Hafezolghorani et al., 2017; Yang et al., 2018; Al-Zuhairi et al., 2022; Tran et al., 2023)**.

Table 6. Ultimate load and deflection at ultimate load: Experimental vs. FEA.

Beam		Ultimate Load (Pu)			Deflection at ultimate load (Δu)		
		EXP(kN)	F.E(kN)	F.E/EXP	EXP(mm)	F.E(mm)	F.E/EXP
Flexural Group	Control BF.C	201.6	195.01	0.9673	30.1	30.4315	1.0110
	BF.S1	220.8	220.417	0.9983	12.67	13.0318	1.0286
	BF.S2	272.1	271.617	0.9982	12.1	13.4604	1.1124
	BF.S3	284.1	282.488	0.9943	11.8	12.0927	1.0248
Shear Group	Control BS.C	510.1	533.751	1.0464	25.1	25.0724	0.9989
	BS.S1	577.2	586.494	1.0161	16.1	17.2252	1.0699
	BS.S2	600.3	601.264	1.0016	15.8	16.6826	1.0559
	BS.S3	629.8	633.92	1.0065	14.99	16.0388	1.0700
Mean				1.004	Mean		1.046
Coefficient of variation (%)				2.216	Coefficient of variation (%)		3.584

The correct simulation of concrete behaviour in a damaged–plasticity model may be achieved by defining damage parameters, such as compressive and tensile damage. Based on concrete damage plasticity (CDP) theory, cracks in RC members are generally formed in regions where the tensile strain exceeds the specified tensile strain of concrete, i.e. the concrete would crack when the plastic strain exceeds zero. In the current investigation, the plastic strain was employed as a representative of crack expansion **(Mahmud et al., 2013; Tysmans et al., 2015; Feng et al., 2018; Faron and Rombach, 2020; Daneshvar et al., 2022).** The cracks appeared orthogonal to the plastic strain. Contour plots in **Figs. 10 and 11** depict the plastic strain distribution in the analyzed beams and the fracture patterns in the experimental beams at the ultimate stage. The influence of strengthening measures on the strain levels and fracture patterns of the flexural and shear groups is adequately shown by these graphic representations. The flexural failure mode was observed in the beams of the flexural group, and the shear failure mode was observed in the beams of the shear group. Additionally, a coincidence fracture pattern was found between the numerical and experimental findings.

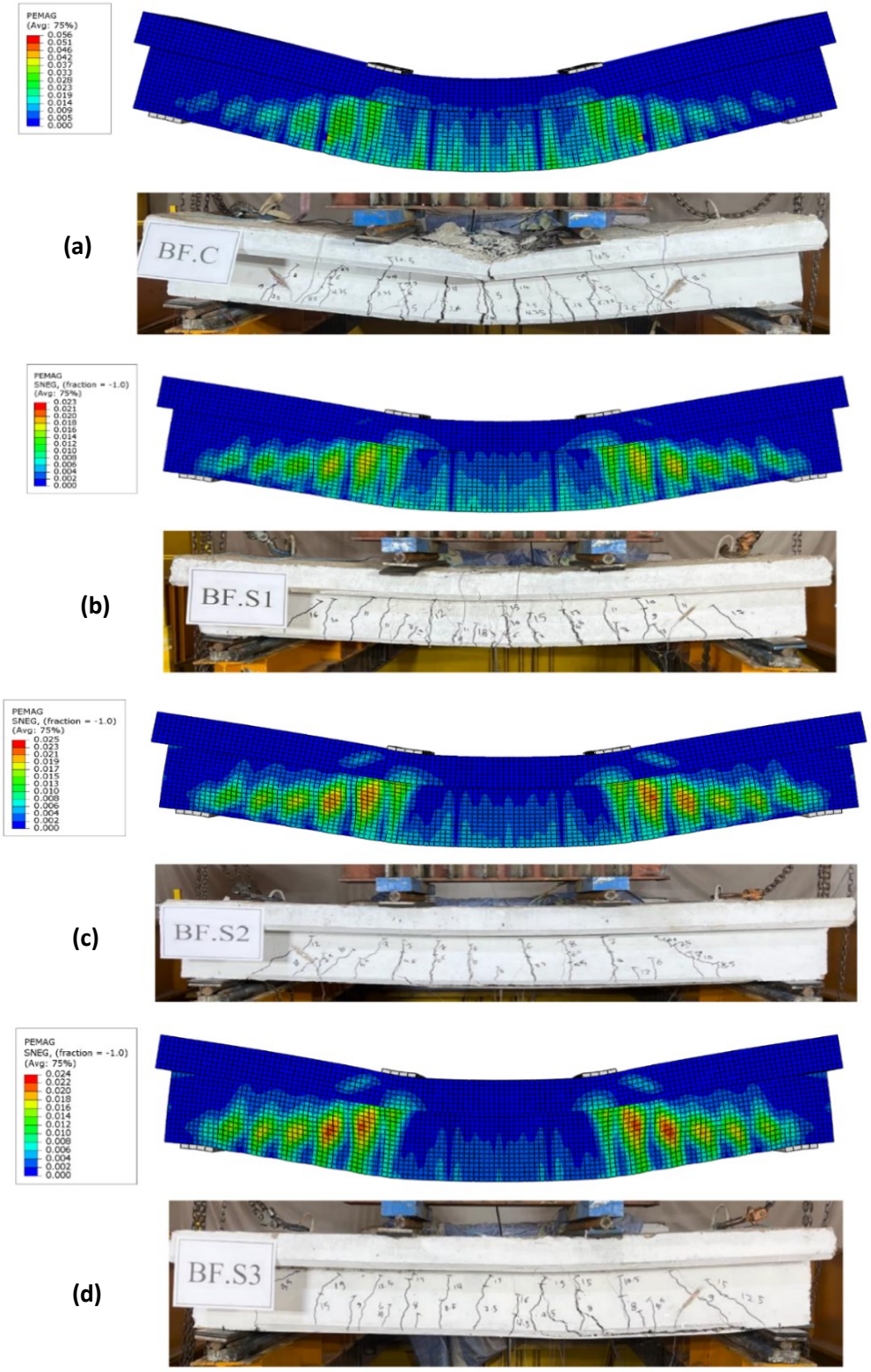

Figure 10. Ultimate damage outcome from ABAQUS simulation and the experiment (flexural group); a) BF.C, b) BF.S1, c) BF.S2 d) BF.S3

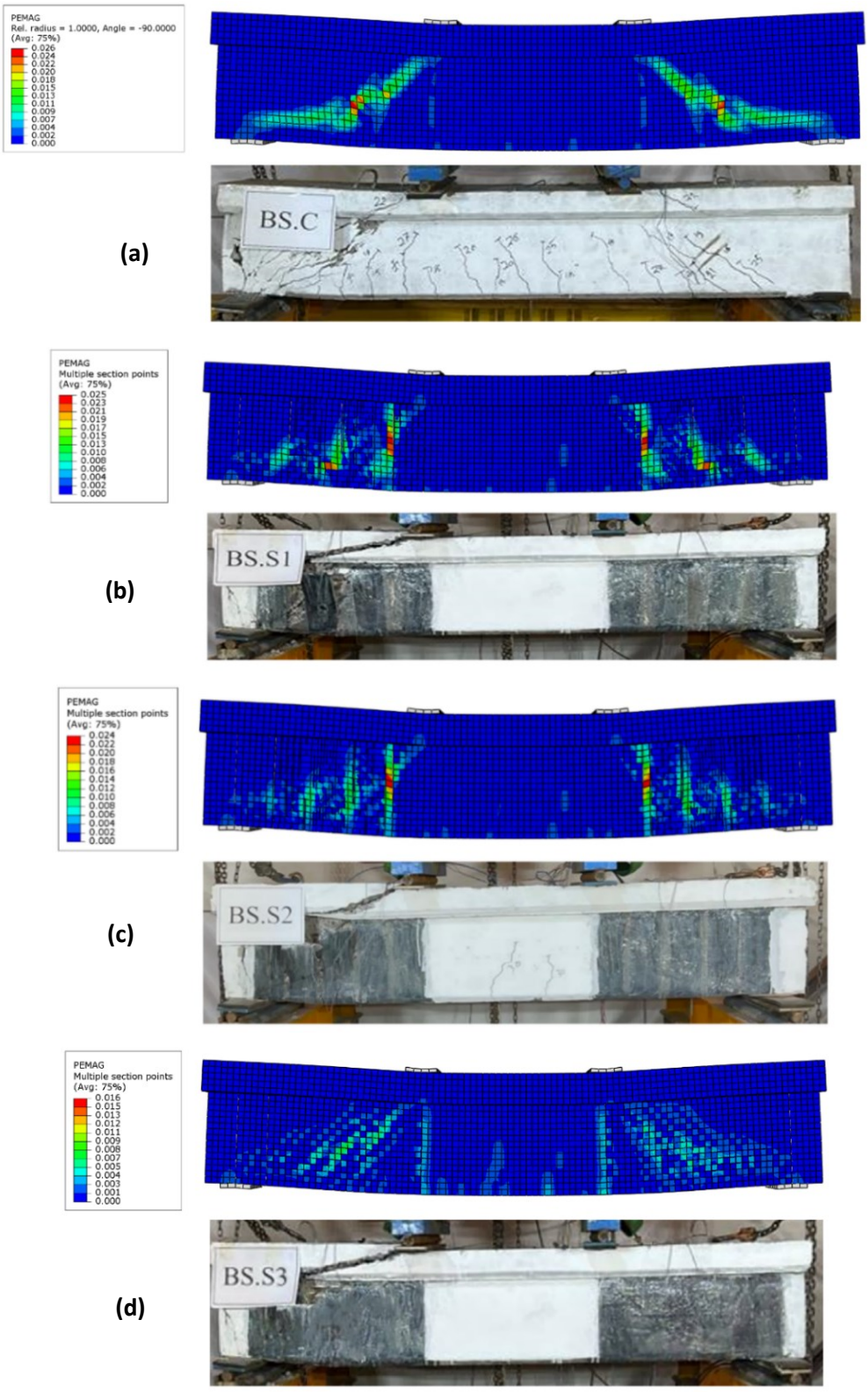

Figure 11. (Continued), Ultimate damage outcome from ABAQUS simulation and the experiment (shear group), a) BF.C, b) BF.S1, c) BF.S2 d) BF.S3

4.3 Numerical Parametric Study

After being verified as suitable for the experimental data, the FEM was used for a comprehensive parametric study of the inclination angle shown by U-CFRP sheets inside the shear group. The impact of the inclination angle of U-CFRP sheets on the beam's structural behaviour was studied using three previous models, BS.S1, BS.S2 and BS.S3, in addition to three new models, BS.DS1, BS.DS2 and BDS.S3, as listed in **Table 7. Fig. 12** shows the creation of parts and assembly in ABAQUS for inclined CFRP models. The effect of the inclination angle of U-CFRP sheets from 90° to 45° on the load–deflection behavior at mid-span is illustrated in **Fig. 13.** Each figure contains a beam with the same spacing as CFRP sheets. According to the load–deflection curves, the beams exhibited equivalent stiffness throughout the elastic range. However, the stiffness characteristics differed after cracking. The beams with inclined CFRP sheets at (45°) had higher shear stiffness than those with vertical CFRP sheets at a similar spacing to CFRP sheets.

Table 7. Details of beams for numerical parametric study.

Beam-ID	The inclination angle of Sheet U-CFRP (degree)	Sheet U-CFRP spacing (mm)
BS.C (ref.)	-	-
BS.S1	90	166
BS.S2	90	125
BS.S3	90	100
BS.DS1	45	166
BS.DS2	45	125
BS.DS3	45	100

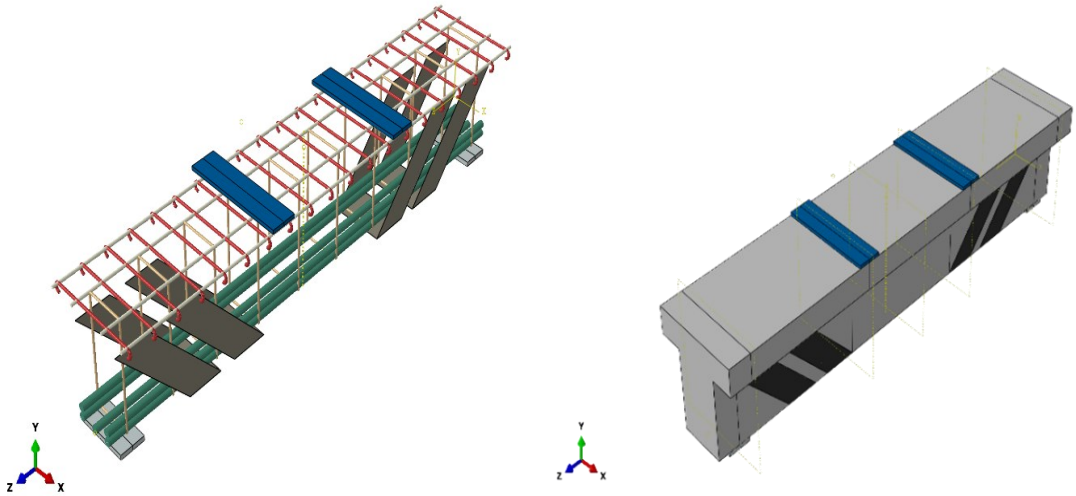

Figure 12. Creating parts and assembly in ABAQUS (inclined CFRP models).

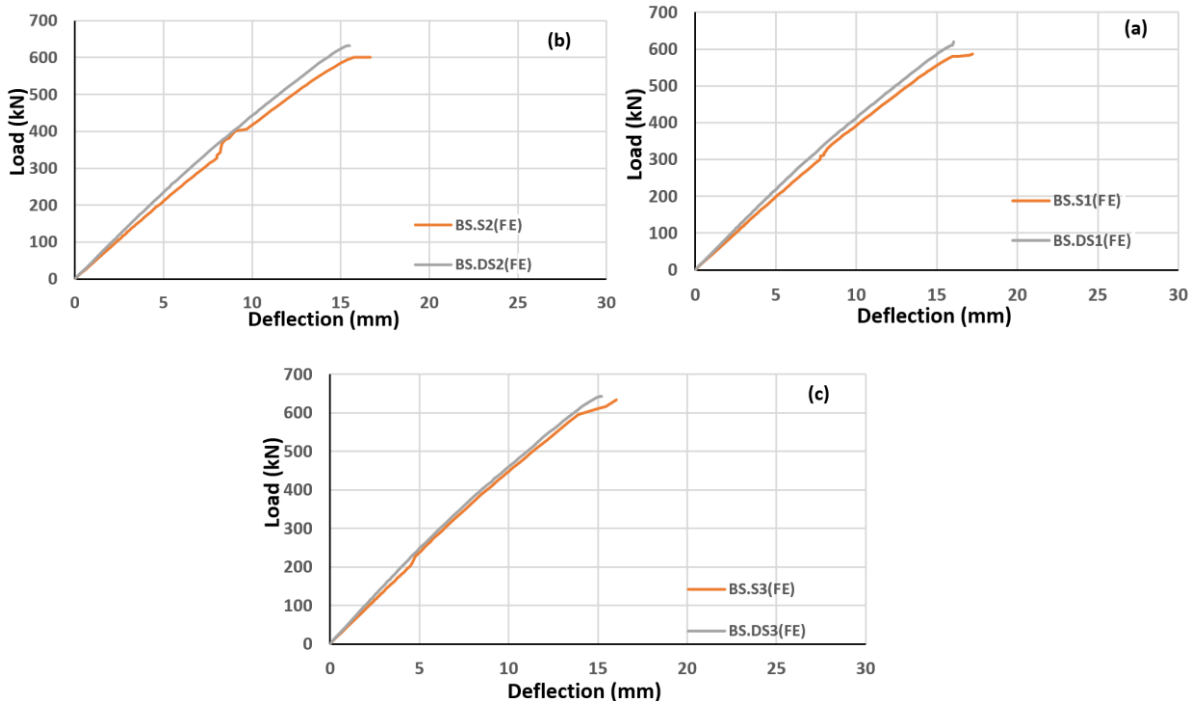

Figure 13. Load–deflection behaviour for the numerical parametric study, a) beams with U-CFRP sheet spacing of 166 mm, b) beams with U-CFRP sheet spacing of 125 mm, c) beams with U-CFRP sheet spacing of 100 mm

Table 8 shows that the beam with inclined CFRP sheets (45°) had an ultimate load higher than the beam with vertical CFRP sheets (90°) with similar spacings of 7.5%, 5.4%, and 2.3%, to the CFRP sheet spacing of 166, 125 and 100 mm, respectively.

Table 8. Ultimate load of beams for numerical parametric study.

Beam-ID	The inclination angle of Sheet U-CFRP (degree)	Sheet U-CFRP spacing (mm)	Pu (kN)	Increasing in Pu (%)	Increase in Pu through changing inclination angle from 90° to 45° (%)
ref. (BS.C)	-	-	510.1	Ref.	-
BS.S1	90	166	577.2	13.2	-
BS.S2	90	125	600.3	17.7	-
BS.S3	90	100	629.8	23.5	-
BS.DS1	45	166	620.5	21.6	7.5
BS.DS2	45	125	632.5	24.0	5.4
BS.DS3	45	100	643.5	26.2	2.2

The ultimate load (Pu) of the beams with vertical CFRP spacing of 166, 125, and 100 mm increased by 13.2%, 17.7%, and 23.5%, respectively, relative to that of the reference beam. The beams with inclined CFRP spacing of 166, 125 and 100 mm exhibited an increase in ultimate load by 21.6%, 24.7%, and 26.2%, respectively, in comparison with the reference beam.

5. CONCLUSIONS

The results were derived from the experiments and analytical simulation. The models were developed to predict the load-bearing capacity of inadequately designed RC T-beams using EB CFRP composites. These composites increased the beam stiffness by increasing the load-carrying capacity and decreasing deflection. The main findings were as follows:

1. A correlation was established between the ultimate load and deflection obtained by the FEA models and experimental methods. Specifically, the mean and coefficient of variation for the ratio of ultimate loads (Pu)FE/(Pu)Exp were 1.004 and 2.216%, respectively. For the ratio of deflection (δ FE/δ Exp), the mean and coefficient of variation were 1.046 and 3.584%, respectively.
2. For the flexural group, a correlation was identified between the width and ultimate bearing capacity of the laminated CFRP. This correlation suggested that the ultimate strength of the laminate increases with its width.
3. The shear resistance of the beams with inclined CFRP sheets at a 45° angle was greater than that of the beams with vertical CFRP sheets, assuming both configurations had a comparable spacing between the CFRP sheets.
4. The beam with inclined CFRP sheets at (45°) had a higher ultimate load-bearing capacity than the beam with vertical CFRP sheets with similar spacing by 7.5%, 5.4%, and 2.3% for the CFRP sheet spacing of 166, 125, and 100 mm, correspondingly.
5. Compared to the reference beam, CFRP increased the ultimate load by 13.2%, 17.7%, and 23.5% for beams with CFRP longitudinal spacing of 166, 125, and 100 mm, respectively . The ultimate load increased by 21.6% ,%24 ,and 26.2% for beams with U-CFRP tilt distances of 166, 125, and 100 mm, respectively.

NOMENCLATURE

Symbol	Description	Symbol	Description
CDP	Concrete damage plasticity theory	FE	Finite element
CFRP	Carbon fiber reinforced polymer	f'_c	Compressive strength of concrete
C3D8R	Brick element	Pu	Ultimate load
EB	Externally bonded	RC	Reinforced concrete
Exp	Experimental	T3D2	The truss element

Acknowledgments

The authors would like to thank the Department of Civil Engineering - University of Baghdad for the support in performing the experimental work and the required analysis.

Credit Authorship Contribution Statement

Hasan Ehssan Alobaidi: Writing the draft, methodology, experimental work, Software, and Validation.
Alaa Hussein Al-Zuhairi: Reviewing, data analysis, proofreading, and supervision.

Declaration of Competing Interest

The authors declare that they have no known competing financial interests or personal relationships that could have appeared to influence the work reported in this paper.

REFERENCES

Abbas, H.Q., and Al-Zuhairi, A.H., 2023. Impact of anchored CFRP composites on the strengthening of partially damaged PC girders. *Journal of Engineering*, *29*(08), pp. 106-120. Doi:10.31026/j.eng.2023.08.08

Abdulhameed, A.A., Al-Zuhairi, A.H., Al Zaidee, S.R., Hanoon, A.N., Al Zand, A.W., Hason, M.M., and Abdulhameed, H.A., 2022. The behavior of hybrid fiber-reinforced concrete elements: A new stress-strain model using an evolutionary approach. *Applied Sciences*, 12(4), P. 2245. Doi:10.3390/app12042245

Abbasi, A., Benzeguir, Z.E.A., Chaallal, O., and El-Saikaly, G., 2022. FE modelling and simulation of the size effect of RC T-beams strengthened in shear with externally bonded FRP fabrics. *Journal of Composites Science*, *6*(4), P. 116. Doi:10.3390/jcs6040116

Alobaidi, H.E., and Al-Zuhairi, A.H., 2023. Structural strengthening of insufficiently designed reinforced concrete T-beams using CFRP composites. *Civil Engineering Journal*, *9*(8), pp. 1880-1896. Doi:10.28991/CEJ-2023-09-08-05

Al Shboul, K.W., Raheem, M.M., and Rasheed, H.A., 2021. Debonding characterization for all-lightweight RC T-beams strengthened in flexure with FRP. *Journal of Building Engineering*, 44(1), P. 103377. Doi:10.1016/j.jobe.2021.103377

Al-Zuhairi, A.H., Al-Ahmed, A.H., Abdulhameed, A.A., and Hanoon, A.N., 2022. Calibration of a new concrete damage plasticity theoretical model based on experimental parameters. *Civil Engineering Journal*, *8*(2), pp. 225-237. Doi:10.28991/CEJ-2022-08-02-03

Abdulhameed, A.A., and Said, A.I., 2019. Behaviour of segmental concrete beams reinforced by pultruded cfrp plates: an experimental study. *Journal of Engineering*, 25(8), pp. 62-79. Doi:10.31026/j.eng.2019.08.11

Buyukozturk, O., Gunes, O., and Karaca, E., 2004, Progress on understanding debonding problems in reinforced concrete and steel members strengthened using FRP composites. *Construction and Building Materials* , 18(1), pp. 9-19. Doi:10.1016/S0950-0618(03)00094-1

Bizindavyi, L., and Neale, K.W., 1999. Transfer lengths and bond strengths for composites bonded to concrete. *ASCE Journal of Composites for Construction*, 3 (4), pp. 153-160. Doi:10.1061/(ASCE)1090-0268(1999)3:4(153)

Benzeguir, Z.E.A., El-Saikaly, G., and Chaallal, O., 2019. Size effect in RC T-beams strengthened in shear with externally bonded CFRP sheets: Experimental study. *Journal of Composites for Construction*, *23*(6), P. 04019048. Doi:10.1061/(ASCE)CC.1943-5614.0000975

Daraj, A.J., and Al-Zuhairi, A.H., 2023. the effect of cohesive debonding elimination on enhancing the flexural performance of damaged unbonded prestressed concrete girders strengthened using NSM CFRP. *Journal of Engineering*, *29*(09), pp. 102-116. Doi:10.31026/j.eng.2023.09.08

Deniaud, C., and Roger Cheng, J.J., 2003. Reinforced concrete T-beams strengthened in shear with fiber reinforced polymer sheets. *Journal of Composites for Construction*, *7*(4), pp. 302-310. Doi:10.1061/(ASCE)1090-0268(2003)7:4(302)

Daneshvar, K., Moradi, M.J., Khaleghi, M., Rezaei, M., Farhangi, V., and Hajiloo, H., 2022. Effects of impact loads on heated-and-cooled reinforced concrete slabs. *Journal of Building Engineering*, 61(1), P. 105328. Doi:10.1016/j.jobe.2022.105328

Faron, A., and Rombach, G.A., 2020. Simulation of crack growth in reinforced concrete beams using extended finite element method. *Engineering Failure Analysis*, 116(1), P. 104698. Doi:10.1016/j.engfailanal.2020.104698.

Feng, D. C., Ren, X. D., and Li, J., 2018. Softened damage-plasticity model for analysis of cracked reinforced concrete structures. *Journal of Structural Engineering*, 144(6), P. 04018044. Doi:10.1061/(ASCE)ST.1943-541X.0002015

Hernoune, H., Benabed, B., Kanellopoulos, A., Al-Zuhairi, A.H., and Guettala, A., 2020. Experimental and numerical study of the behaviour of reinforced masonry walls with NSM CFRP strips subjected to combined loads. *Buildings*, *10*(6), P. 103. Doi:10.3390/buildings10060103

Hafezolghorani, M., Hejazi, F., Vaghei, R., Jaafar, M.S.B., and Karimzade, K., 2017. Simplified damage plasticity model for concrete. *Structural Engineering International*, 27(1), pp. 68-78. Doi:10.2749/101686616X1081

Ibrahim, R.S., and Al-Zuhairi, A.H., 2022. Behaviour of RC columns strengthened by combined (CFRP and steel jacket). *Materials Today: Proceedings*, *61*, pp. 1126-1134. Doi:10.1016/j.matpr.2021.10.514

Elwi, A.A., and Murray, D.W., 1979. A 3D hypoelastic concrete constitutive relationship. *Journal of the Engineering Mechanics Divi*sion, 105(4), pp. 623-641. Doi:10.1061/JMCEA3.0002510

Hordijk, D.A., and Reinhardt, H.W., 1991. Growth of discrete cracks in concrete under fatigue loading. In Toughening mechanisms in quasi-brittle materials (pp. 541-554). Dordrecht: Springer Netherlands. Doi:10.1007/978-94-011-3388-3_33

Lorenzis, L., Miller, B., and Nanni, A., 2001. Bond of fiber-reinforced polymer laminates to concrete. *ACI material journal*, 98 (1), pp. 256-264. Doi:10.14359/10281

Mhanna, H.H., Hawileh, R.A., and Abdalla, J.A. 2019. Shear strengthening of reinforced concrete beams using CFRP wraps. *Procedia Structural Integrity*, 17, pp. 214-221. Doi:10.1016/j.prostr.2019.08.029

Mahmud, G.H., Yang, Z., and Hassan, A.M., 2013. Experimental and numerical studies of size effects of Ultra High Performance Steel Fibre Reinforced Concrete (UHPFRC) beams. *Construction and Building materials*, 48(1), pp. 1027-1034. Doi:10.1016/j.conbuildmat.2013.07.061

Naqi, A.W., and Al-zuhairi, A.H., 2020. Nonlinear finite element analysis of RCMD beams with large circular opening strengthened with CFRP material. *Journal of Engineering*, 26(11), pp. 170-183. Doi:10.31026/j.eng.2020.11.11

Nakaba, K., Kanakubo, T., Furuta, T., and Yoshizawa, H., 2001. Bond behaviour between fiber-reinforced polymer laminates and concrete. *ACI Structural Journal*, 98 (3), pp. 359-367. Doi:10.14359/10224

Najaf, E., Orouji, M., and Ghouchani, K., 2022. Finite element analysis of the effect of type, number, and installation angle of FRP sheets on improving the flexural strength of concrete beams. *Case Studies in Construction Materials*, 17(1), P. 01670. Doi:10.1016/j.cscm.2022.e01670

Nicolaides, D., and Markou, G., 2015. Modelling the flexural behaviour of fibre reinforced concrete beams with FEM. *Engineering Structures*, 99, pp. 653-665. Doi:10.1016/j.engstruct.2015.05.028

Shah, S.A.R., Khan, A.R., Aslam, M.A., Khan, T., Arshad, K., Hussan, S., Sultan, A., Shahzadi, G., and Waseem, M., 2020. Sustainable FRP-confined symmetric concrete structures: an application experimental and numerical validation process for reference data. *Applied Sciences*, 10(1), P. 333. Doi:10.3390/app10010333

Singh, M., Sheikh, A.H., Ali, M.M., Visintin, P., and Griffith, M.C., 2017. Experimental and numerical study of the flexural behaviour of ultra-high performance fibre reinforced concrete beams. Construction and Building Materials, 138, pp. 12-25. Doi:10.1016/j.conbuildmat.2017.02.002

Tran, D.A., Shen, X., Sorelli, L., Ftima, M.B., and Brühwiler, E., 2023. Predicting the effect of non-uniform fiber distribution on the tensile response of ultra-high-performance fiber reinforced concrete by magnetic inductance-based finite element analysis. *Cement and Concrete Composites*, 135(1), P. 104810. Doi:10.1016/j.cemconcomp.2022.104810

Tysmans, T., Wozniak, M., Remy, O., and Vantomme, J., 2015. Finite element modelling of the biaxial behaviour of high-performance fibre-reinforced cement composites (HPFRCC) using Concrete Damaged Plasticity. *Finite Elements in Analysis and Design*, 100, pp. 47-53. Doi:10.1016/j.finel.2015.02.004

Ueda, T., Sato, Y., and Asano, Y., 1999. experimental study on bond strength of continuous carbon fiber sheet. *ACI,SP.,* 188 (37), pp. 407-413. Doi:10.14359/5641

Yang, X., Liu, L., and Wang, Y., 2018. Experimental test and numerical simulation of the initial crack reinforced concrete beam in bending. In IOP Conference Series: Earth and Environmental Science, 186(2), P. 012056. Doi:10.1088/1755-1315/186/2/012056

Zaki, M.A., Rasheed, H.A., Roukerd, R.R., and Raheem, M., 2020. Performance of reinforced concrete T beams strengthened with flexural CFRP sheets and secured using CFRP splay anchors. *Engineering Structures*, 210(1), P. 110304. Doi:10.1016/j.engstruct.2020.110304

Zhang, D., Wang, Q., and Dong, J., 2016. Simulation study on CFRP strengthened reinforced concrete beam under four-point bending. *Computers and Concrete*, 17(3), pp. 407-421. Doi:10.12989/cac.2016.17.3.407